Inorganic Chemistry

Article

pubs.acs.org/IC

Self-Assembled Supramolecular Clusters Based on Phosphines and Coinage Metals: Tetrahedra, Helicates, and Mesocates

Sang Ho Lim and Seth M. Cohen*

Department of Chemistry and Biochemistry, University of California, San Diego, La Jolla, California 92093, United States

Supporting Information

ABSTRACT: An array of coordination-driven supramolecular metal−ligand clusters has been synthesized using polytopic phosphine ligands and coinage metals (Cu^+, Ag^+, Au^+). Rigid 3-fold or 2-fold symmetric phosphine ligands have been prepared: 1,3,5-tris((4-(diphenylphosphino)ethynyl)phenyl)-benzene) (tppepb, $\mathbf{L^1}$), 1,4-bis((diphenylphosphino)ethynyl)benzene (1,4-dppeb, $\mathbf{L^2}$), 1,3-bis((diphenylphosphino)ethynyl)benzene (1,3-dppeb, $\mathbf{L^3}$), 2,6-bis((diphenylphosphino)ethynyl)pyridine (2,6-dppep, $\mathbf{L^4}$), and 1,5-bis-((diphenylphosphino)ethynyl)naphthalene (1,5-dppen, $\mathbf{L^5}$). Self-assembly of these ligands with coinage metals produces four different types of metal−ligand clusters, or in some cases coordination polymers, depending on number and relative geometry of the phosphine donor atoms. Supramolecular tetrahedral clusters of the formula $M_4(\mathbf{L^1})_4I_4$ (M = Cu^+, Ag^+, Au^+) were obtained with the tppepb ligand, encapsulating solvent molecules (either CH_2Cl_2 or DMF) as guests within the central cavity of the clusters. The ligands 1,3-dppeb ($\mathbf{L^3}$) and 2,6-dppep ($\mathbf{L^4}$) give achiral, triple-stranded, dinuclear mesocates with the formula $M_2(\mathbf{L})_3I_2$ (M = Cu^+ or Au^+). In contrast, the ligand 1,4-dppeb ($\mathbf{L^2}$) generates a triple-stranded, dinuclear helicate with Cu^+, but a coordination polymer with Au^+ (both with the empirical formula $M_2(\mathbf{L^2})_3I_2$). Finally, coordination polymers were obtained from 1,5-dppen ($\mathbf{L^5}$) with Cu^+. The clusters have been fully characterized by single crystal X-ray crystallography, high-resolution mass spectrometry, ^{1}H NMR, and ^{31}P NMR.

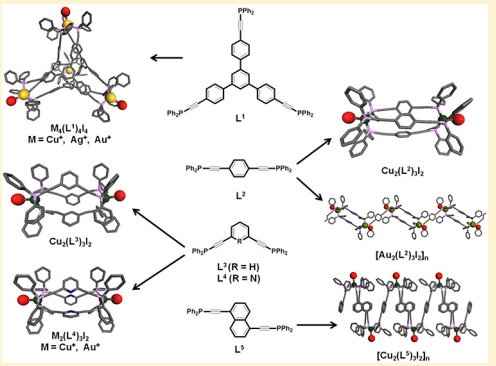

INTRODUCTION

Supramolecular metal−ligand clusters, sometimes referred to as metal−organic polyhedra (MOPs), have been an area of great interest over the past few decades.[1] These clusters combine polydentate organic ligands and transition metals to form elegant assemblies held together by reversible metal−ligand bonds. The coordination preferences of the metal ion combined with the directionality encoded in the ligand geometry can direct the formation of clusters of varying geometries. Supramolecular architectures including helicates,[2] tetrahedra,[3] octahedra,[4] dodecahedra,[5] cuboctahedra,[6] and many others[7] have been obtained from these coordination-driven self-assembly reactions. The laboratories of Fujita, Raymond, Stang, and others have shown that these clusters can demonstrate spectacular host−guest chemistry, including molecular encapsulation and recognition,[8] stabilization of reactive molecules and intermediates,[9] and cavity controlled catalytic reactions.[10] The majority of these clusters reported in the literature involve metal ions coordinated by polydentate ligands that utilize nitrogen and/or oxygen donor atoms.[1]

In light of the vast literature on these types of self-assembled structures, it is somewhat surprising that relatively few constructs have been assembled from soft Lewis base ligands, such as those derived from second row heteroatoms (e.g., S, P, etc.). These ligands would be expected to form stable assemblies in conjunction with lower oxidation state metal ions or metalloids (i.e., soft Lewis acids). One example from Hahn and co-workers is the preparation of helicates, mesocates, and tetrahedra from bis(benzene-*o*-dithiol),[11] tris(benzene-*o*-dithiol),[12] and mixed benzene-*o*-dithiolato/catecholato derivatives.[13] The Hahn group has also investigated cylinder-shaped supramolecular structures combining polydentate N-heterocyclic carbene (NHC), as softer carbon-based ligands, in combination with coinage metal ions.[14] Johnson and co-workers have also used thiol-based ligands to obtain self-assembled clusters based on As^{3+}, Sb^{3+}, Bi^{3+}, and P^{3+}.[15]

Among soft Lewis base ligands that could be used for these assemblies, phosphines are particularly attractive, having played crucial roles in the development of coordination chemistry and homogeneous catalysis since the 1960s.[16] Although phosphines have been widely investigated in coordination chemistry, particularly with late transition metals, their use as building blocks in supramolecular clusters remains quite limited compared to other N- and O-donor ligands. This may be due to the bulky substituents and irregular shapes often associated with phosphine ligands, which can lead to more complicated geometries and lower predictability of forming well-defined supramolecular assemblies.[17] However, some supramolecular assemblies have been described with phosphine ligands,[2f,18] including many from the group of Puddephatt, who have reported elegant examples of both discrete and infinite

Received: December 24, 2012

   dx.doi.org/10.1021/ic302840x | *Inorg. Chem.* XXXX, XXX, XXX−XXX

Scheme 1. Synthetic Scheme for Each of the Supramolecular Assemblies Obtained with Rigid Phosphine Ligands: $M_4(L^1)_4I_4$ Tetrahedron, $M_2(L^2)_3I_2$ Helicate, $M_2(L^3)_3I_2$ and $M_2(L^4)_3I_2$ Mesocates, and $[M_2(L^2)_3I_2]_n$ and $[M_2(L^5)_3I_2]_n$ Coordination Polymers

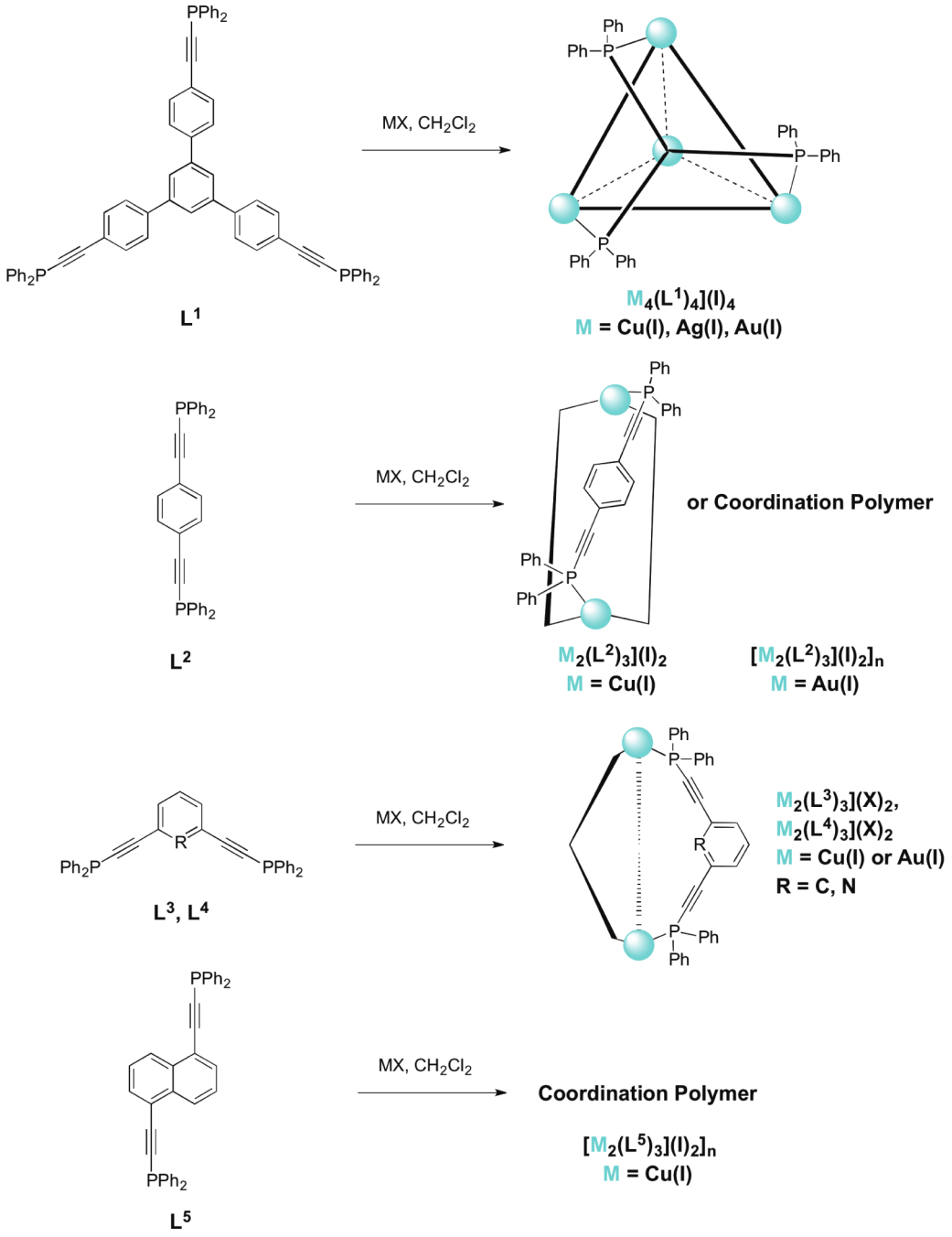

assemblies.[18a] The groups of Yip[18b] and James[18c] have also prepared self-assembled structures from phosphine ligands with coinage metals Ag^+ or Au^+ to obtain rings, helicates, and a small, adamantoid-shaped cluster. In one instance, Yip and co-workers obtained a homoleptic, trinuclear ring structure composed of three bridging 9,10-bis(diphenylphosphino)-anthracene ligands and three Au^+ ions with a ClO_4^- anion guest in the center.[18b] In another example, the group of James obtained the M_6L_4 "superadamantoid" cage $[Ag_6(CH_3C(CH_2PPh_2)_3)_4(OTf)_4](OTf)_2$ using a flexible, triphosphine $CH_3C(CH_2PPh_2)_3$ ligand.[18c]

Phosphine ligands have many attractive features for use in supramolecular clusters, including the applicability of ^{31}P NMR spectroscopy, interesting luminescent properties (with certain metal ions),[18d,19] and their relevance to organometallic chemistry and homogeneous catalysis.[20] Also, the softer donor character of phosphines may produce more stable clusters because of the additional covalency in the bonding with lower oxidation state metal ions. In light of these features, we previously reported the first phosphine-based supramolecular tetrahedra clusters,[21] which were made by the combination of coinage metals Cu^+, Ag^+, or Au^+ with the rigid, 3-fold symmetric ligand 1,3,5-tris((4-(diphenylphosphino)ethynyl)-

dx.doi.org/10.1021/ic302840x | Inorg. Chem. XXXX, XXX, XXX–XXX

benzene) (tppeb). These tetrahedra were found to be persistent in solution as shown by ESI-MS, ^{1}H NMR, and ^{31}P NMR analysis.

The aforementioned Platonic clusters were generated by the formation of 4-coordinate, tetrahedral metal ions centers with three phosphine donors and a coordinated iodide ion. The persistence of this coordination motif across all three coinage metals (i.e., Cu^+, Ag^+, Au^+) suggested that related clusters could be accessed with a variety of ligands, metal ions, and counterions. Therefore, we sought to prepare other phosphine ligands that would produce supramolecular clusters of different symmetry and sizes. Herein, we show that the combination of di- and tritopic phosphine ligands and coinage metals can form a variety of supramolecular cluster motifs including tetrahedral $M_4L_4I_4$ clusters, dinuclear $M_2L_3I_2$ triple-stranded helicates, dinuclear $M_2L_3I_2$ triple-stranded mesocates, and $[M_2L_3I_2]_n$ coordination polymers. Soluble species have been characterized in solution by high-resolution mass spectrometry, ^{1}H NMR, and ^{31}P NMR. The present study represents one of the most extensive studies on phosphine-based supramolecular architectures and shows the substantial potential of such ligands to participate in self-assembled coordination clusters.

RESULTS AND DISCUSSION

Ligand Synthesis. The synthesis of the ligands, tppepb ($\mathbf{L^1}$), 1,4-dppeb ($\mathbf{L^2}$), 1,3-dppeb ($\mathbf{L^3}$), 2,6-dppep ($\mathbf{L^4}$), and 1,5-dppen ($\mathbf{L^5}$) was achieved using literature procedures (Supporting Information, Schemes S1 and S2). Using standard Sonogashira coupling methods,[22] the aryl halides 1,3,5-tris(4-bromophenyl)benzene, 1,4-dibromobenzene, 2,6-dibromopyridine, and 1,5-diiodonaphthalene were combined with trimethylsilyl acetylene in the presence of $PdCl_2(PPh_3)_2$/CuI or $Pd(PPh_3)_4$/CuI catalyst. The corresponding terminal alkynes were obtained by the hydrolysis of the TMS groups under basic conditions. Adapting the method of Constable et al.,[23] the corresponding terminal alkyne compounds were treated with ^{n}BuLi and Ph_2PCl in freshly dried tetrahydrofuran (THF) to give reasonable yields of the desired ligands $\mathbf{L^1}$–$\mathbf{L^5}$.

Tetrahedral Clusters $M_4(L^1)_4I_4$ (M = Cu^+, Ag^+, and Au^+). A summary of all of the supramolecular clusters obtained is provided in Scheme 1. To obtain expanded, tetrahedral clusters, a 1:1 suspension of a coinage metal iodide and the ligand $\mathbf{L^1}$ were combined in CH_2Cl_2 for 30 min at room temperature, resulting in the formation of a colorless solution. This solution was filtered and evaporated to dryness. Slow diffusion of Et_2O into a saturated solution of the isolated powders in CH_2Cl_2 gave colorless crystals in high yield (~80% from the powder) within a few days. Alternatively, crystals could also be prepared from a saturated (hot) DMF solution of the powder, upon standing at room temperature for approximately one week. The X-ray crystal structures of all three tetrahedral clusters, crystallized from CH_2Cl_2, are shown in Figure 3 (Supporting Information, Table S1). All of the clusters crystallize in centrosymmetric space groups and generally are very similar (Figure 1). In all of the clusters, the phosphine ligands occupy a pyramidalized, 3-fold symmetric coordination around the M^+ coinage metal. The overall geometry of the M^+ ions is tetrahedral, with the apical site occupied by a tightly bound iodide ligand. The average metal-phosphine distances in the clusters are 2.28, 2.52, and 2.39 Å in the Cu^+, Ag^+, and Au^+ clusters, respectively. Similarly, the average metal-iodide distances are 2.56, 2.75, and 2.82 Å in the Cu^+, Ag^+, and Au^+ clusters, respectively (Supporting Information, Table S4). The

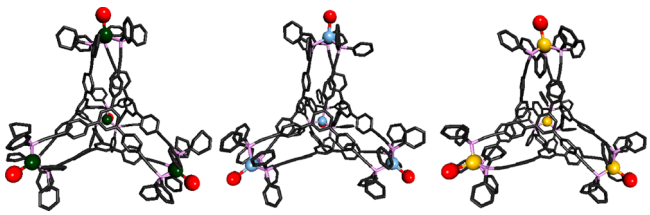

Figure 1. Crystal structures of the $M_4(\mathbf{L^1})_4I_4$ tetrahedra. Each cluster is shown with the ligand as sticks and the M^+ ions and iodide anions as colored spheres: Cu^+ (dark green), Ag^+ (light blue), Au^+ (yellow), and I^- (red).

metal-phosphine and metal-iodide bond distances are in good agreement with those of metal-phosphine and metal-iodide bonds in other four-coordinate phosphine-based M^+ iodide complexes.[24] The ligand design and cluster architecture enforce that all of the metal ions adopt a single, identical chiral configuration, making the overall cluster chiral. However, as expected, both enantiomers of the cluster are present in the crystal related by inversion symmetry. Each cluster has a distinct packing pattern (Supporting Information, Figure S1), with the $Au_4(\mathbf{L^1})_4I_4$ cluster showing strong π–π stacking interactions (3.68 Å) between the central benzene rings of the $\mathbf{L^1}$ ligands of adjacent clusters (no such interactions are observed for the Cu^+ and Ag^+ clusters in the solid state). One ligand of $Au_4(\mathbf{L^1})_4I_4$ is distorted inwardly, making the cavity volume slightly reduced compared to other clusters (322, 326, and 312 Å^3 for Cu^+, Ag^+, and Au^+, respectively).[25]

In our earlier communication,[21] the $M_4(tppeb)_4I_4$ (M = Cu^+, Ag^+, and Au^+) tetrahedra showed no evidence of guest binding, presumably because of the rather small cavity volume (129, 133, 135 Å^3 for Cu^+, Ag^+, Au^+, respectively). In contrast, the tetrahedral clusters presented here have relatively large cavity volumes (vide supra) and subsequently one CH_2Cl_2 solvent molecule is located inside the cavity in all cases. Based on intermolecular distances, there are close C–H···π contacts (~2.68, 2.54, 2.52 Å for Cu^+, Ag^+, Au^+, respectively) between the aromatic walls of the cluster and the hydrogen atoms of the solvate molecule (CH_2Cl_2) within the cluster cavity. Other small molecules could be encapsulated; for example when crystallized from hot DMF, a DMF solvent molecule was found inside the cavity of $Ag_4(tppeb)_4I_4$ (Figure 2, Supporting Information,Table S1). However, no close contacts were observed between encapsulated DMF and the aromatic walls of the cluster. It is unclear at this stage what the driving force

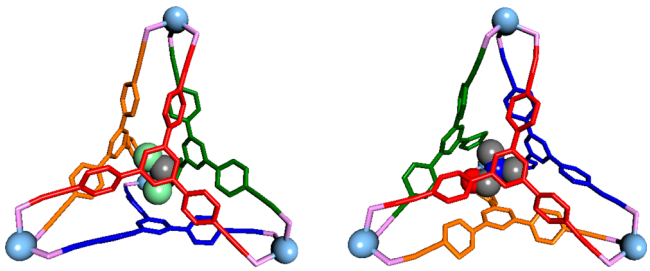

Figure 2. Crystal structure of $Ag_4(\mathbf{L^1})_4I_4$ with either encapsulated CH_2Cl_2 (left) or DMF (right). The cluster geometry of $Ag_4(\mathbf{L^1})_4I_4$ is highlighted by removing the phenyl groups and iodide ions, and coloring each ligand differently. The Ag^+ ions and the guest molecules are shown in spacefilling representation.

dx.doi.org/10.1021/ic302840x | Inorg. Chem. XXXX, XXX, XXX–XXX

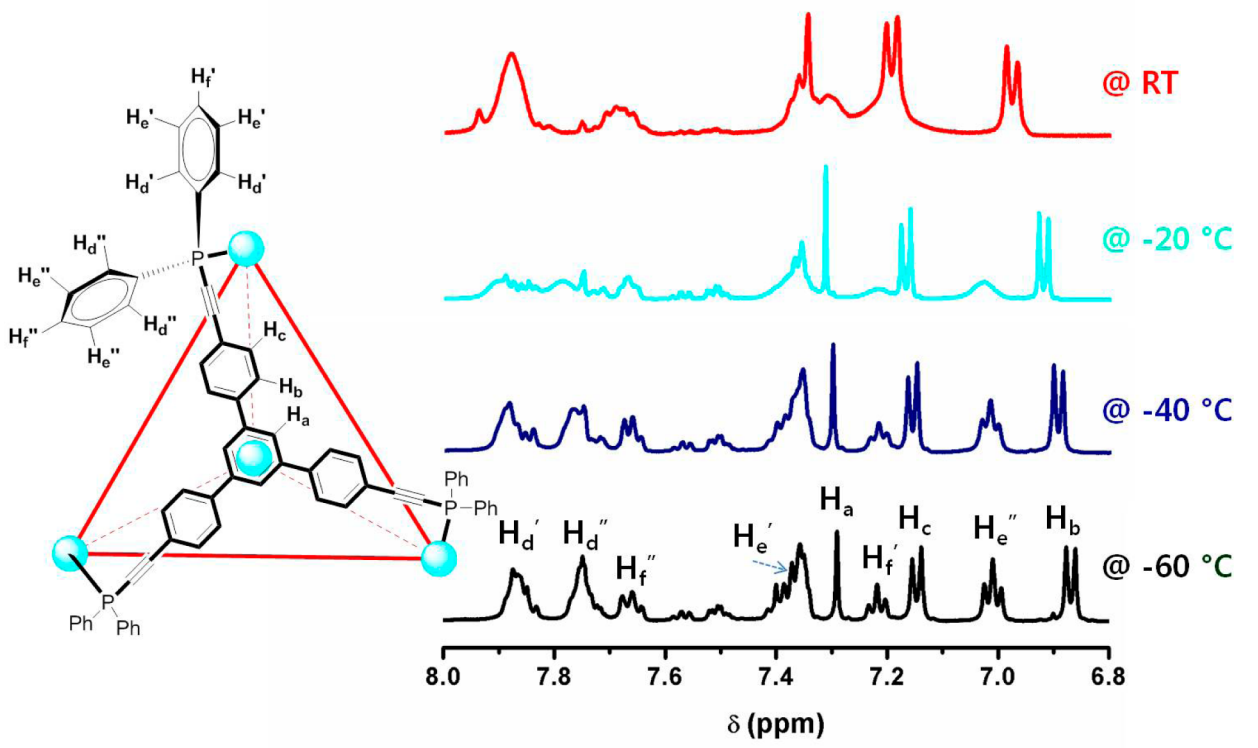

Figure 3. Variable temperature ^{1}H NMR spectra of $Ag_4(L^1)_4I_4$ in CD_2Cl_2.

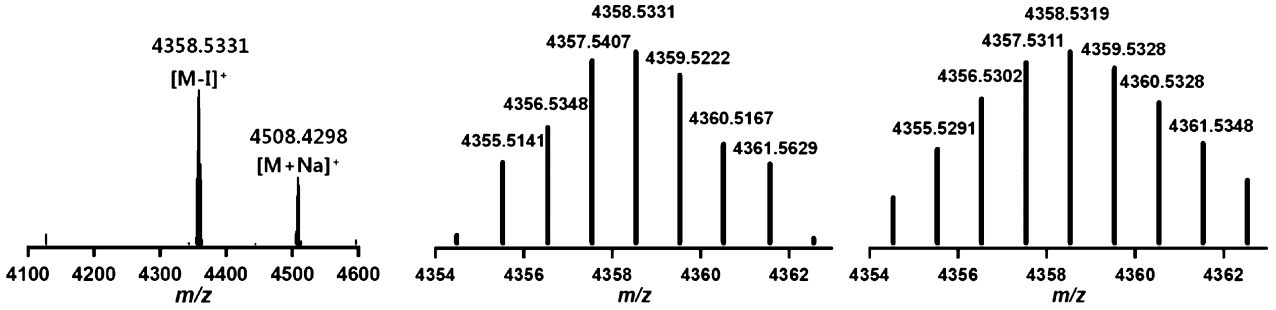

Figure 4. High-resolution ESI-MS of $Cu_4(L^1)_4I_4$. The positive ion mode experimental (left), magnification of the $[M-I]^+$ base peak (middle), and the simulated $[M-I]^+$ (right) spectra are shown.

for encapsulation of these molecules is, but it may simply involve weak dispersion forces.

To examine their persistence in solution, ^{1}H NMR and ESI-MS analysis of these clusters was performed. Unlike the previously reported $M_4(tppeb)_4I_4$ tetrahedra, a spectrum of $Ag_4(L^1)_4I_4$ collected at room temperature (25 °C) shows several sharp signals arising from the central benzene ring and 1,3,5-phenyl groups and very broad signals from the phenyl groups on phosphorus atoms (Figure 3). The singlet at 7.29 ppm (H_a) and doublets at 6.86 and 7.14 ppm (H_b and H_c) are attributed to the central benzene ring and 1,3,5-phenyl groups in L^1, respectively. The broad signals of the phenyl protons are attributed to dynamic motions. Variable temperature NMR studies were performed (Figure 3), which showed that the broad signals become more resolved as the temperature is decreased down to −60 °C. In particular, proton signals at −60 °C indicate an asymmetry between the phenyl rings on each phosphorus atom (two distinct environments for $H_{e'}$ and $H_{e''}$ at δ = 7.01, 7.36 ppm; and for $H_{f'}$ and $H_{f''}$ at δ = 7.22, 7.66 ppm). These signals were assigned based on the spectra of $M_4(tppeb)_4I_4$, which were fully assigned by a COSY NMR experiment.[21] Unfortunately, numerous attempts to obtain variable temperature ^{1}H NMR of the other clusters (Cu^+ and Au^+), using several different deuterated solvents ($CDCl_3$, d^6-DMF, d^6-acetone etc.), did not produce well-resolved spectra (data not shown).

^{31}P NMR of the each cluster showed a distinct peak (δ = 7.73, −31.38, 7.99 ppm for Cu^+, Ag^+, and Au^+ for respectively, Supporting Information, Figure S2), and the peak of the free ligand (L^1) is no longer present. The chemical shift of the Ag^+ cluster appears at a chemical shift close to that of the free ligand, but is clearly distinct in terms of its expected splitting patterns by ^{107}Ag−P and ^{109}Ag−P couplings ($^1J(^{107}Ag-P)$ = 246 Hz and $^1J(^{109}Ag-P)$ = 284 Hz). Strangely, the chemical shift is quite different from nearly all the other clusters examined in this study. Although we do not have any reasonable explanation why the signal of the Ag^+ cluster is so shifted compared to those of Cu^+ and Au^+ clusters (Supporting Information, Figure S2), the ^{31}P NMR chemical shifts of phosphine complexes can vary depending on metal, anions, and

dx.doi.org/10.1021/ic302840x | Inorg. Chem. XXXX, XXX, XXX−XXX

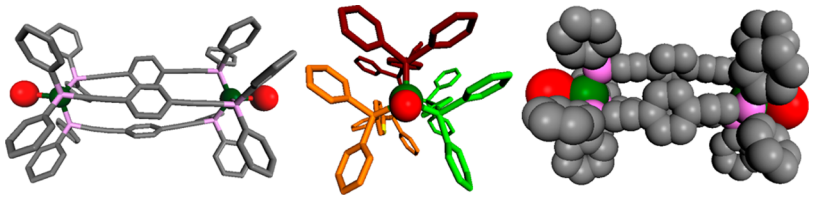

Figure 5. Three views of the $Cu_2(L^2)_3I_2$ helical cluster, shown with the ligand as sticks and the Cu^+ ions and iodide anions as spheres (left); the cluster geometry is highlighted coloring each ligand differently viewed down the Cu−Cu axis (middle); and shown in spacefill (right).

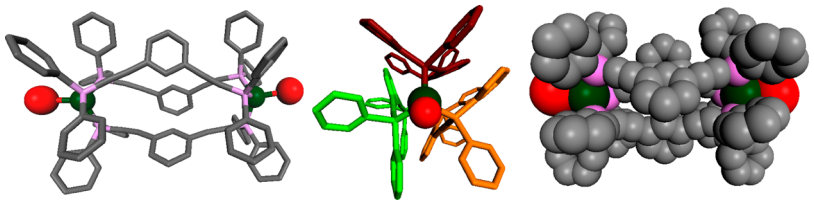

Figure 6. Three views of the $Cu_2(L^3)_3I_2$ pseudomesocate cluster: shown with the ligand as sticks and the Cu^+ ions and iodide anions as spheres (left); the cluster geometry is highlighted by coloring each ligand differently as viewed down the Cu···Cu axis (middle); and shown in spacefill (right).

even coordination number. For instance, some complexes such as $[M_2(dppb)_2]X_2$ (M = Ag^+ or Au^+, dppb = bis-(diphenylphosphino)butane) complexes have significantly different chemical shifts.[26] In $[Au_2(dppb)_2]X_2$,[26a,b] the values are +41.5 and +35.6 ppm for X = BF_4^- and I^-, respectively. However, those of $[Ag_2(dppb)_2]X_2$[26c] are −15.6, −5.0, and +0.8 ppm for X = Br^-, I^-, and NO_3^-, respectively. On the other hand, the signals of $M((p\text{-tolyl})_3P)_nCl$ (M = Au^+ or Ag^+ and n = 1, 2, 3, or 4),[27] appear in a similar region (δ = 31.32 for $Au((p\text{-tolyl})_3P)Cl$[27a] and δ = 21.4−25.3 ppm for $Ag((p\text{-tolyl})_3P)_nCl$).[27b] Although the ^{31}P NMR spectra do not suggest whether each cluster exists in solution with certainty, the spectra do suggest that a single species exists in solution of each cluster. In the case of $Cu_4(L^1)_4I_4$, the solution composition is further supported by the positive ion mode ESI-MS spectra of $Cu_4(L^1)_4I_4$ (Figure 4), which shows two peaks indicative of the intact cluster ($[Cu-I]^+$ m/z 4358.5331, $[Cu+Na]^+$ m/z 4508.4298). Unfortunately, the Ag^+ and Au^+ clusters did not yield ESI-MS spectra with the expected ions.

Helical Cluster $Cu_2(L^2)_3I_2$. A series of ditopic phosphine ligands were prepared to evaluate whether M_2L_3 triple-stranded helicates (or mesocates) or possibly M_4L_6 tetrahedra could be produced.[1a] Combining 2 equiv of CuI in CH_2Cl_2 with 3 equiv of linear ligand L^2 for 30 min at room temperature resulted in the formation of a colorless solution, which was filtered and evaporated to dryness to obtain a powder. Slow diffusion of Et_2O into a saturated CH_2Cl_2 solution prepared from the isolated powder gave colorless crystals in high yield (∼90%). The single crystal X-ray structure determination reveals that the product is a triple-stranded helicate, which was anticipated by analogy to other supramolecular systems. Similar to the tetrahedral clusters, the metal centers adopt distorted tetrahedral environments at each metal center (Figure 5) coordinated by an iodide anion (Cu−I distance ∼2.64 Å) and by three phosphine donor atoms from three separate ligands (Cu−P distance ∼2.30 Å) (Supporting Information, Table S5). The tetrahedral coordination environments of the metal centers are homochiral, as required by their helical symmetry. The average helical twist angle is 23.57° about the Cu−Cu axis of the molecule (as taken from the Cu−P−P−Cu torsion angles, Supporting Information, Figure S3). The length of the helix, as defined by the intranuclear Cu···Cu distance, is ∼12.9 Å (Supporting Information,Table S5). The twelve phenyl groups located on the exterior of the helix arrange efficiently in offset face-to-face stacked pairs.

The solution structure of $Cu_2(L^2)_3I_2$ was examined by ^1H NMR spectroscopy (Supporting Information, Figure S4). In the ^1H NMR spectrum, the proton signal of free ligand L^2 appears largely as broad multiplets between 7.3 and 7.7 ppm; however, $Cu_2(L^2)_3I_2$ displays a relatively simple and well-resolved peak pattern as expected for a highly symmetric cluster that is intact in solution. The structural integrity in solution is supported by the ^{31}P NMR spectrum of $Cu_2(L^2)_3I_2$, where the peak of the free L^2 ligand (−33.85 ppm) is no longer present and a new resonance at 9.84 ppm is observed (Supporting Information, Figure S5). Finally, high resolution ESI-MS data confirmed the presence of the cluster in solution. The positive ion mode ESI-MS spectrum of $Cu_2(L^2)_3I_2$ shows several ions indicative of the fully intact cluster (Supporting Information, Figure S6), including ions at m/z of 1737.1703 and 1887.0631 correspond to the $[M-I]^+$ and $[M+Na]^+$ exact masses (consistent with the simulated isotopic spectrum). Additional peaks in the ESI-MS correspond to the $[M+K]^+$ (m/z 1903.0631) and $[M+Cu]^+$ (m/z 1927.0060) ions. The combination of ligand L^2 with AgI was also performed; however, no suitable crystals were obtained under a variety of conditions. ^1H NMR, ^{31}P NMR, and ESI-MS studies of the reaction mixture did not produce conclusive results. In particular, uncoordinated free ligand (L^2) was observed in the ^{31}P NMR spectrum under the reaction conditions explored (δ = −33.85, data not shown). Interestingly, the combination of Au^+ with ligand L^2 yielded a compound with the same stoichiometry as $Cu_2(L^2)_3I_2$, but formed a coordination polymer $[Au_2(L^2)_3I_2]_n$ rather than a discrete helicate (vide infra). It is unclear why Ag^+ and Au^+ do not produce the analogous helicate structures. The affinity of these metal ions for phosphine ligands may make the equilibrium between the solution and crystalline states of the material more complicated. As a result, the kinetic, rather than thermodynamic products, may be the products isolated by crystallization.

Mesocate Cluster $Cu_2(L^3)_3I_2$. Using the linear ditopic phosphine ligand L^2, a helical cluster was selectively formed

dx.doi.org/10.1021/ic302840x | Inorg. Chem. XXXX, XXX, XXX−XXX

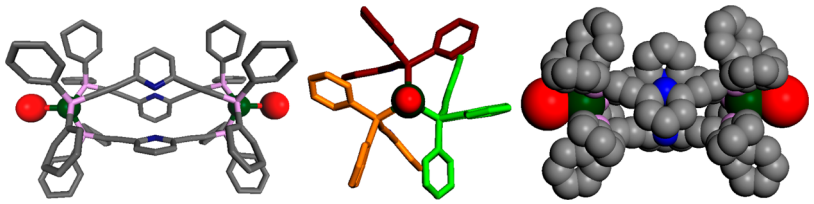

Figure 7. Three views of the $Cu_2(L^4)_3I_2$ mesocate cluster: shown with the ligand as sticks and the Cu^+ ions and iodide anions as spheres (left); the cluster geometry is highlighted by coloring each ligand differently as viewed down the Cu···Cu axis (middle); and shown in spacefill (right).

both in solution and in the solid-state with Cu^+. Ligand L^3 possess a bent (1,3-benzene), rather than a linear (1,4-benzene for L^2), geometry and hence was expected to produce related, but structurally distinct clusters. It was anticipated that the bent linker of L^3 would lead to syn conformations at the metal centers because of geometric constraints (this is in contrast to L^2, which can accommodate syn, anti, and even intermediate conformations).

The mesocate of $Cu_2(L^3)_3I_2$ was prepared in a similar manner to that for $Cu_2(L^2)_3I_2$, and crystals were obtained by slow diffusion of Et_2O into a saturated CH_2Cl_2 solution (~70% yield) within two weeks. In contrast to $Cu_2(L^2)_3I_2$, the single crystal X-ray structure of $Cu_2(L^3)_3I_2$ reveals a heterochiral, triple-stranded mesocate (Figure 6, Supporting Information,Table S2) with the metal centers possessing opposite chirality. However, the $Cu_2(L^3)_3I_2$ complex is not an idealized mesocate structure. Each Cu^+ center has a slightly different coordination environment (Supporting Information,Table S5); the average twist angle is about 5.59° about the Cu···Cu axis of the molecule (as taken from the Cu−P−P−Cu torsion angles, Supporting Information, Figure S3), which is smaller than that of $Cu_2(L^2)_3I_2$. The intramolecular Cu···Cu distance in $Cu_2(L^3)_3I_2$ is slightly smaller (ca. 12.1 Å) than that in $Cu_2(L^2)_3I_2$ because of the structure of the substituted ligand (1,3- vs 1,4-substitution on the central benzene ring, Supporting Information,Table S5). Interestingly, the central benzene ring of each ligand participates in a face-to-edge interaction with respect to the neighboring ligand.

In solution, the $Cu_2(L^3)_3I_2$ cluster behaves as an idealized mesocate. Only one set of signals for all three ligands is obtained, indicating C_3 symmetry for the complexes in solution, at room temperature, on the NMR time scale (Supporting Information, Figure S7). In particular, only one singlet signal for the central benzene proton (H_a) appears and is shifted dramatically upfield (5.64 ppm) compared to the free ligand (7.72 ppm). This upfield shift is characteristic of a proton experiencing a ring current shielding due to edge-to-face interactions as observed in the X-ray crystal structure. Similar to the $Cu_2(L^2)_3I_2$ cluster, the signals for the phenyl rings attached to each phosphorus atom appear as broad multiplets at 7.80 ppm (H_d), a triplet at 7.30 ppm (H_f), and a triplet at 7.16 ppm (H_e) (Supporting Information, Figure S7). The positive ion mode ESI-MS spectrum of $Cu_2(L^3)_3I_2$ shows two distinct peaks, also confirming that the cluster remains intact in solution (m/z = 1737.1673, 1887.0631 for $[M-I]^+$ and $[M+Na]^+$, respectively, Supporting Information, Figure S8). Numerous attempts to obtain suitable crystals for the other coinage metal ions (Ag^+, Au^+) were not successful, and ^1H NMR data of the corresponding reaction mixtures were inconclusive. In the ^{31}P NMR spectra of the reaction mixtures containing either Ag^+ or Au^+, the peak of the free L^3 ligand (−34.06 ppm) was absent and several new peaks (δ = 30.86, 6.47 for Ag^+, and δ = 6.03, −13.72 for Au^+) were observed, indicative of several species in the solutions (Supporting Information, Figure S9). Analysis by ESI-MS revealed that the reaction with Au^+ gave peaks indicative of $Au_2(L^3)_3I_2$ (m/z = 2004.2507 for $[M-I]^+$, Supporting Information, Figure S10), but the reaction with Ag^+ did not yield expected ions.

Mesocate Cluster $M_2(L^4)_3I_2$, (M = Cu^+, Au^+). Because of the observed edge-to-face interaction in the mesocate cluster $Cu_2(L^3)_3I_2$, it was predicted that introducing a 2,6-pyridine linker would eliminate the pore-facing hydrogen atoms and would be expected to construct mesocate clusters with more idealized symmetry. Indeed, higher symmetric mesocate clusters $M_2(L^4)_3I_2$, (M = Cu^+, Au^+) were successfully isolated in a similar manner to that of $Cu_2(L^2)_3I_2$. Slow diffusion of Et_2O into a saturated CH_2Cl_2 solution of the compounds gave yellow crystals in near quantitative yield (>95%). Similar to $Cu_2(L^3)_3I_2$, the structure reveals $M_2(L^4)_3I_2$ are triple-stranded mesocates (Figure 7, Supporting Information, Figure S11). The clusters with Cu^+ and Au^+ are essentially isostructural, possessing C_{3h} symmetry (C_3 symmetry along the metal-to-metal axis and a σ_h mirror plane) such that only one-sixth of the cluster resides in the crystallographic asymmetric unit (Supporting Information,Table S2). Consequently, the coordination environments of metal centers are identical to each other, bound by three identical phosphorus atoms (M^+−P distance 2.28 and 2.38 Å for Cu^+ and Au^+, respectively) and an iodide ion (M^+−I distance 2.57 and 2.79 Å for Cu^+ and Au^+, respectively). The M···M separations in each $M_2(L^4)_3I_2$ are similar, at 12.12 and 12.00 Å for Cu^+ and Au^+, respectively (Supporting Information,Table S5).

The ^1H NMR spectra of the $M_2(L^4)_3I_2$ clusters show only one set of signals for the ligand protons, indicating C_3 symmetry for the complexes in solution on the NMR time scale (Supporting Information, Figure S12). In the Cu^+ cluster, distinct upfield shifts of the protons on the central pyridine ring are observed ($\Delta\delta$ = +1.18 and +0.67 compared to the free ligand). Similar, but smaller shifts, are found for the Au^+ cluster ($\Delta\delta$ = +0.61 and +0.14), which suggest that these protons are involved in face-to-edge aromatic interactions between adjacent pyridine rings in solution. The ^{31}P NMR spectrum supported the solution presence of both clusters (Supporting Information, Figure S13), where the peak of the free L^3 ligand (−34.06 ppm) was no longer present and a new resonance was observed for the clusters $M_2(L^4)_3I_2$ (Cu^+ δ = 9.64 ppm; Au^+ δ = 10.06 ppm). The positive ion mode ESI-MS spectrum of $Cu_2(L^4)_3I_2$ shows two distinct peaks, confirming the presence of the cluster in solution (m/z = 1740.1607 and 1890.0528 for $[M-I]^+$ and $[M+Na]^+$, respectively, Supporting Information, Figure S14). We were unable to obtain a clean ESI-MS spectrum of $Au_2(L^4)_3I_2$. As in the L^2 and L^3 ligand systems, we were unable to obtain suitable crystals upon combination of L^4 and Ag^+, and spectroscopic studies of the reaction mixture were inconclusive.

dx.doi.org/10.1021/ic302840x | Inorg. Chem. XXXX, XXX, XXX−XXX

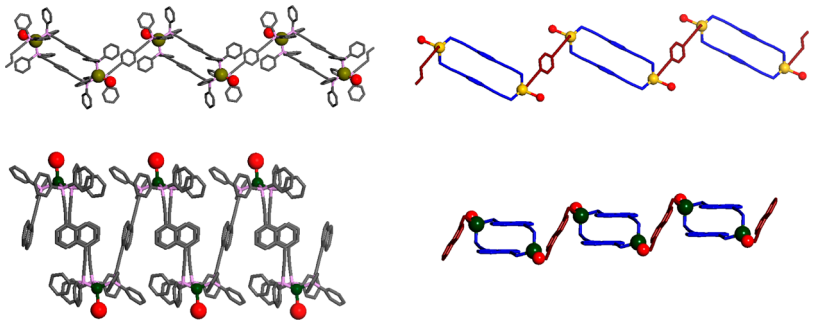

Figure 8. Two views of the $[Au_2(L^2)_3I_2]_n$ (top) and $[Cu_2(L^5)_3I_2]_n$ (bottom) coordination polymers: the ligands are shown as sticks and the M^+ ions and iodide anions are represented by spheres (left); the cluster geometry is highlighted coloring each ligand differently with the phenyl groups excluded (right).

Coordination Polymer $[Au_2(L^2)_3I_2]_n$. Although the ligand−metal combinations described above generally led to the anticipated supramolecular structures, other combinations yielded products, but not the expected structures. As mentioned above, unlike the results with the tppeb[21] or L^1 ligand, many of the ditopic ligand systems did not give the same supramolecular structures across the entire coinage metal series. One example was the combination of Au^+ with ligand L^2, which yielded a compound with the same stoichiometry as $Cu_2(L^2)_3I_2$, but rather than a discrete helicate was a coordination polymer $[Au_2(L^2)_3I_2]_n$. Suitable crystals of $[Au_2(L^2)_3]I_2]_n$ were obtained from slow diffusion of Et_2O into a saturated CH_2Cl_2 solution after one day. The crystals showed poor solubility in most common organic solvents, and the structure clearly showed an extended coordination polymer (Figure 8) consisting of $Au_2(L^2)_2I_2$ dimer units, which are linked into one-dimensional chains by a third, bridging L^2 ligand. The Au···Au distances are ∼13.1 Å across the $Au_2(L^2)_2I_2$ dimer unit and ∼14.4 Å across the single L^2 bridge (Supporting Information,Table S6). Within the $Au_2(L^2)_2I_2$ dimer, two nearly parallel L^2 ligands participate in a $\pi-\pi$ stacking interaction with a face-to-face distance of ∼3.9 Å between the centers of the benzene rings. The two distinct types of L^2 ligands in the structure (dimer versus bridging ligand) adopt different conformations in the coordination polymer as reflected in the Au−P−P−Au torsion angles (Supporting Information,Table S6). The dimer ligands adopt a nearly gauche conformation (torsion angle = 62.79°), but the third, bridging ligand adopts an anti conformation (torsion angle = 180°).

Although the coordination polymer $[Au_2(L^2)_3]I_2]_n$ shares the same stoichiometry with the helicate $Cu_2(L^2)_3I_2$, attempts to obtain the analogous $Au_2(L^2)_3I_2$ helicate were not successful. Variable temperature ^{1}H NMR and ESI-MS analysis suggest the $Au_2(L^2)_3I_2$ helicate, or related discrete species, may be present in solution. Dissolution of the coordination polymer crystals in CD_2Cl_2 using extensive sonication (because of the poor solubility of the crystals) resulted in broad, overlapping signals at room temperature (Supporting Information, Figure S15). However, these broad signals became resolved as the temperature was decreased to −60 °C. Interestingly, the spectrum at −60 °C shows a highly symmetric pattern, distinct from the free L^2 ligand (Supporting Information, Figure S15). The spectra at −60 °C is very similar to that obtained for the helicate $Cu_2(L^2)_3I_2$ (Supporting Information, Figure S4), indicating that a similar $Au_2(L^2)_3I_2$ structure may be formed in solution at low temperature. The ^{1}H NMR data is supported by positive ion mode ESI-MS, which shows several peaks consistent with a helicate in solution (Supporting Information, Figure S16). A peak at m/z 2004.2443 corresponds to the exact mass of the molecular ion minus an iodide ion (i.e., $[M-I]^+$), which confirms the molecular formula of the cluster. Additional peaks in the ESI-MS correspond to the $[M+H]^+$ (m/z 2132.1525) and $[M+Au]^+$ (m/z 2328.1127), all of which suggests the existence of the $Au_2(L^2)_3I_2$ cluster in solution (Supporting Information, Figure S16).

These results beg the question as to why the coordination polymer $[Au_2(L^2)_3I_2]_n$ is selectively crystallized rather than the dinuclear cluster. An earlier study by James and co-workers examined the transformation of M_2L_3 cages into $[M_2L_3]_n$ polymers. It was suggested that the transformation might occur through ring-opening polymerization arising from the equilibrium between the solution and crystalline states of the material. In solution the discrete cage was dominant but was in equilibrium with a coordination polymer (or oligomers). The polymeric form was insoluble and slowly and irreversibly crystallized out of solution. The insolubility of the polymer leads to crystallization, and the rate-determining factor was reported to be the ring-opening polymerization reaction, rather than the crystallization.[28] It appears that a similar equilibrium and crystallization mechanism is occurring for the $[Au_2(L^2)_3I_2]_n$ coordination polymer described above.

Coordination Polymer $[Cu_2(L^5)_3I_2]_n$. One of the most studied supramolecular clusters, reported by Raymond and co-workers, uses a bis(catecholato) ligand with an intervening naphthalene spacer. This backbone causes the catechol binding units to be offset from one another, thus disfavoring the formation of a helicate, and forming an M_4L_6 tetrahedron with extensive host−guest properties.[29] It was hoped that a bis(phosphine) ligand with an identical naphthalene (L^5) backbone would generate a similar cluster. However, combination L^5 with Cu^+ ions produced a coordination polymer very similar to $[Au_2(L^2)_3I_2]_n$. Suitable crystals for single crystal X-ray diffraction were prepared from a saturated (hot) DMF solution of the complex upon cooling to room temperature. The crystals obtained were insoluble in most common organic solvents. X-ray diffraction reveals the crystal structure is a coordination polymer with the formula $[Cu_2(L^5)_3I_2]_n$. (Figure 8). Similar to $[Au_2(L^2)_3I_2]_n$, the structure consists of $[Cu_2(L^5)_2I_2]$ dimer units with distorted tetrahedral Cu^+ centers, which are linked into polymer chains by a third, bridging L^5 ligand. The Cu···Cu distances are ∼13.7 Å within the $[Cu_2(L^5)_2I_2]$ dimer and ∼14.8 Å between the L^5 bridged centers (Supporting Information,Table S6). In the $[Cu_2(L^5)_2I_2]$ unit, the two, nearly parallel L^5 ligands have $\pi-\pi$

dx.doi.org/10.1021/ic302840x | Inorg. Chem. XXXX, XXX, XXX−XXX

stacking interactions at a distance of ~3.7 Å between the naphthyl rings. The dimer and bridging ligands adopt gauche and anti conformations, respectively (Supporting Information,Table S6), as described for $[Au_2(\mathbf{L}^2)_3I_2]_n$. It appears that the lack of a chelating ligand, combined with the propensity for these ligands to engage in strong $\pi-\pi$ stacking interactions does not allow for access to the tetrahedral structure. In essence, the ability to obtain an analogue to the spectacular M_4L_6 tetrahedron reported by Raymond is not readily accessed by simply adopting the naphthyl backbone strategy to a substantially different ligand system.

CONCLUSIONS

In summary, phosphine coordination chemistry has mainly focused on organometallics and homogeneous catalysis. Only occasionally have they been considered as building blocks for supramolecular chemistry and self-assembly. However, a new class of supramolecular metal-phosphine clusters formed from tritopic/ditopic phosphines and coinage metals has been developed. The structures obtained include tetrahedra, dinuclear triple-stranded helicates, dinuclear triple-stranded mesocates, and coordination polymers. While tetrahedral clusters could be obtained with all of the coinage metals (Cu^+, Ag^+, Au^+) when using tritopic tris(phosphine) ligands, the same was not true when employing ditopic bis(phosphine) ligands. For reasons as yet to be determined, Ag^+ ions were found to be particularly challenging when trying to isolate supramolecular species. Different geometries of bis(phosphine) ligands lead to helicates, mesocates, or coordination polymers, all of which share a common stoichiometry $[M_2(\mathbf{L})_3I_2]_n$. The growing use of coinage metal-phosphine complexes as catalysts[30] suggest these clusters might serve as unusual scaffolds not only for new catalyst design and but also for investigating the catalytic behaviors of the new types of phosphine-based discrete and polymeric aggregates.

EXPERIMENTAL SECTION

General Procedure. Starting materials and solvents were purchased and used without further purification from commercial suppliers (Sigma-Aldrich, Alfa Aesar, Acros, TCI, Cambridge Isotope Laboratories, Inc., and others). ^{1}H and ^{31}P nuclear magnetic resonance (NMR) spectra were recorded by a Varian FT-NMR spectrometer (400 MHz for ^{1}H) or JEOL FT-NMR spectrometer (500 MHz for ^{1}H/202.468 MHz for ^{31}P). Phosphorus nuclear magnetic resonance spectroscopy was fully decoupled by broadband decoupling. Chemical shifts were quoted in parts per million (ppm) referenced to the appropriate solvent peak or 0 ppm for TMS (^{1}H NMR) and −6 ppm for triphenylphosphine solution in $CDCl_3$ (^{31}P NMR).

1,3,5-Tris[4-(2-trimethylsilyl-ethynyl)phenyl]benzene (1). 1,3,5-Tris(4-bromophenyl)benzene (5.0 g, 9.2 mmol) was dissolved in diethylamine (350 mL) under an atmosphere of nitrogen. CuI (32 mg, 0.6 mol %/Br) and $PdCl_2(PPh_3)_2$ (240 mg, 1.2 mol %/Br) were added to the solution. Trimethylsilylacetylene (13.7 mL, 33 mmol) was slowly added, and the mixture was heated to reflux at 50 °C for 12 h. Once conversion was complete (by TLC), the solvent was evaporated. The mixture was separated by silica gel column chromatography (*n*-Hexane) to isolate the title compound (4.64 g, 85%). ^{1}H NMR ($CDCl_3$, 400 MHz): δ 7.74 (s, 3H), 7.63(d, 6H, J = 8 Hz), 7.57(d, 6H, J = 8 Hz), 0.28 (s, 27H).

1,3,5-Tris-(4-ethynylphenyl)benzene (2). Compound **1** (4.5 g, 7.56 mmol) was dissolved in 60 mL of CH_2Cl_2, followed by addition of a mixture of MeOH/NaOH (60 mL/1.8 g). The mixture was stirred for 12 h at room temperature. Once conversion was complete (by TLC), the solvent was evaporated. 50 mL of CH_2Cl_2 was added to the residue, and the insoluble solids were filtered away. The filtrate was washed with brine (2 × 20 mL) and then, the organic phase was separated and dried with Na_2SO_4. After removing the solvent, the solid mixture was separated by silica gel column chromatography using CH_2Cl_2 as eluent to give the title compound (2.63 g, 92%). ^{1}H NMR ($CDCl_3$, 400 MHz): δ 7.76 (s, 3H), 7.65 (d, 6H, J = 8 Hz), 7.61 (d, 6H, J = 8 Hz), 3.16(s, 3H); ^{13}C NMR (150 MHz, $CDCl_3$): δ 141.7, 141.1, 132.7, 127.2, 125.3, 121.6, 83.4, 78.1. ESI-MS (+) m/z calcd. for $[M+MeOH+H]^+$: 411.17, found $[M+MeOH+H]^+$: 411.32.

1,3,5-Tris[(4-(diphenylphosphino)ethynyl)phenyl]benzene ($\mathbf{L}^1$). Compound **2** (3.91 g, 10.33 mmol) was dissolved in freshly dried THF (150 mL) at −20 °C. ^{n}BuLi (2.5 M hexane, 14.9 mL, 37.2 mmol) was added to the solution. The reaction mixture was stirred for 30 min, and then Ph_2PCl (6.7 mL, 37.2 mmol) was added and the mixture stirred for an additional 1 h. Once reaction was complete (by TLC), the solvent was evaporated, and the residue was dissolved in CH_2Cl_2 (50 mL). The organic layer was washed with water (2 × 30 mL). After drying with Na_2SO_4, the solvent was removed in a vacuum to yield a pale yellow solid which was recrystallized (CH_2Cl_2/MeOH) at 0 °C to give the title compound (7.31 g, 76%). ^{1}H NMR ($CDCl_3$, 400 MHz): δ 7.80 (s, 3H), 7.69−7.74 (br s, 24H), 7.39−7.41 (br s, 18H); ^{31}P NMR ($CDCl_3$, 202.468 MHz): δ −33.88. ESI-MS(+) m/z calcd. for $[M+H]^+$: 931.28, found $[M+H]^+$: 931.47.

1,4-Bis[(2-trimethylsilyl)ethynyl]benzene (3). 1,4-Dibromobenzene (7.02 g, 30 mmol) was dissolved in triethylamine (100 mL) under an atmosphere of nitrogen. CuI (136 mg, 1.2 mol %/) and $Pd(PPh_3)_4$ (420 mg, 0.6 mol %) were added to the solution. Trimethylsilylacetylene (10.3 mL, 72 mmol) was slowly added, and the mixture was heated to reflux for 8 h. Once conversion was complete (by TLC), the solvent was evaporated. The mixture was separated by silica gel column chromatography (*n*-hexane) to isolate the title compound (7.30 g, 90%). ^{1}H NMR ($CDCl_3$, 400 MHz): δ 7.39 (s, 4H), 0.25 (s, 18H); ^{13}C NMR(150 MHz, $CDCl_3$): δ 131.73, 123.11, 96.28, 95.10, −0.11.

1,4-Diethynylbenzene (4). Compound **3** (5.4 g, 20 mmol) was dissolved in 60 mL of CH_2Cl_2, followed by addition of a mixture of MeOH/NaOH (60 mL/3.2 g). The mixture was stirred for 12 h at room temperature. Once conversion was complete (by TLC), the solvent was evaporated. 50 mL of CH_2Cl_2 was added to the residue, and the insoluble solids were filtered away. The filtrate was washed with brine (2 × 30 mL), and the organic phase was separated and dried with Na_2SO_4. After removing the solvent, the solid mixture was separated by silica gel column chromatography using CH_2Cl_2 as eluent, and the title compound was obtained (2.30 g, 91%). ^{1}H NMR ($CDCl_3$, 400 MHz): δ 7.44 (s, 4H), 3.17(s, 2H). ESI-MS (+) m/z calcd. for $[M+H_2O+H]^+$: 145.07, found $[M+H_2O+H]^+$: 145.09, calcd. for $[M+MeOH+H]^+$: 159.08, found $[M+MeOH+H]^+$: 159.17.

1,4-Bis[(diphenylphosphino)ethynyl]benzene ($\mathbf{L}^2$). Compound **4** (3.8 g, 30.0 mmol) was dissolved in freshly dried THF (100 mL) at −20 °C. ^{n}BuLi (2.5 M hexane, 28.8 mL, 72.0 mmol) was slowly added to the solution. The reaction mixture was stirred for 30 min, and then Ph_2PCl (12.9 mL, 72.0 mmol) was added and the mixture stirred for an additional 1 h. Once reaction was complete (by TLC), the solvent was evaporated, and the residue was dissolved in CH_2Cl_2 (50 mL). The organic layer was washed with water (2 × 30 mL). After drying with Na_2SO_4, the solvent was removed in vacuum to give a white solid that was recrystallized (CH_2Cl_2/MeOH) at 0 °C to give the title compound (12.9 g, 87%). ^{1}H NMR ($CDCl_3$, 400 MHz): δ 7.63−7.67 (br s, 8H), 7.49 (s, 4H), 7.35−7.37 (br s, 12H); ^{31}P NMR ($CDCl_3$, 202.468 MHz): δ −33.85. ESI-MS(+) m/z calcd. for $[M+H]^+$: 495.14, found $[M+H]^+$: 495.36.

1,3-Bis[(diphenylphosphino)ethynyl]benzene ($\mathbf{L}^3$). The 1,3-diethynylbenzene (1.05 mL, 7.9 mmol) was dissolved in freshly dried THF (30 mL) at 253 K. ^{n}BuLi (2.5 M hexane, 7.6 mL, 19.0 mmol) was added to the solution. The reaction mixture was stirred for 30 min, and then Ph_2PCl (3.4 mL, 19.0 mmol) was added and the mixture stirred for an additional 1 h. Once reaction was complete (by TLC), the solvent was evaporated, and the residue was dissolved in CH_2Cl_2 (50 mL). The organic layer was washed with water (2 × 30 mL). After drying with Na_2SO_4, the solvent was removed in a vacuum to yield a yellow oil (3.4 g, 87%). ^{1}H NMR ($CDCl_3$, 400 MHz): δ 7.72 (s, 1H),

dx.doi.org/10.1021/ic302840x | Inorg. Chem. XXXX, XXX, XXX−XXX

7.64−7.69 (br s, 8H), 7.51(d, 2H, J = 8 Hz), 7.35−7.39 (br s, 12H), 7.32 (t, 1H, J = 8 Hz) ; ^{31}P NMR ($CDCl_3$, 202.468 MHz): δ −34.06 . ESI-MS(+) m/z calcd. for $[M+H]^+$: 495.14, found $[M+H]^+$: 495.27.

2,6-Bis[(trimethylsilyl)ethynyl]pyridine (5). 2,6-Dibromopyridine (1.18 g, 5 mmol) was dissolved in diethylamine (50 mL) under an atmosphere of nitrogen. CuI (11 mg, 0.6 mol %) and $PdCl_2(PPh_3)_2$ (84 mg, 1.2 mol %/Br) were added to the solution. Trimethylsilylacetylene (1.7 mL, 12 mmol) was slowly added, and the mixture was heated to reflux for 8 h. Once conversion was complete (by TLC), the solvent was evaporated. The solid mixture was separated by silica gel column chromatography (n-hexane:CH_2Cl_2, 1:4) to isolate the title compound (1.15 g, 85%). ^{1}H NMR ($CDCl_3$, 400 MHz): δ 8.58(br s, 2H), 7.81 (t, 1H, J = 2.4 Hz), 0.25 (s, 18H).

2,6-Diethynylpyridine (6). Compound **5** (1.02 g, 3.76 mmol) was dissolved in 20 mL of CH_2Cl_2, followed by addition of a mixture of MeOH/NaOH (10 mL/1.5 g). The mixture was stirred for 12 h at room temperature. Once conversion was complete (by TLC), the solvent was evaporated. Twenty millilters of CH_2Cl_2 was added to the residue, and the insoluble solids were filtered away. The filtrate was washed with brine (2 × 30 mL), and the organic phase was separated and dried over Na_2SO_4. After removing the solvent, the mixture was separated by silica gel column chromatography using CH_2Cl_2 as eluent to give the title compound (0.45 g, 94%). ^{1}H NMR ($CDCl_3$, 400 MHz): δ 8.65 (d, 2H, J = 2 Hz), 7.85 (t, 1H, J = 2 Hz), 3.24 (s, 2H); ESI-MS (+) m/z calcd. for $[M+H]^+$: 128.05, found $[M+H]^+$: 128.13, calcd. for $[M+MeOH+H]^+$: 160.08, found $[M+MeOH+H]^+$: 160.11.

2,6-Bis[(diphenylphosphino)ethynyl]pyridine (L^4). Compound **6** (0.45, 3.54 mmol) was dissolved in freshly dried THF (30 mL) at −20 °C. ^{n}BuLi (2.5 M hexane, 3.40 mL, 8.49 mmol) was slowly added to the solution. The reaction mixture was stirred for 30 min, and then Ph_2PCl (1.5 mL, 8.49 mmol) was added and the mixture was stirred an additional 2 h. Once reaction was complete (by TLC), the solvent was evaporated, and the residue was dissolved in CH_2Cl_2 (30 mL). The organic layer was separated and washed with water (3 × 20 mL). After drying with Na_2SO_4, the solvent was removed in vacuum to give a yellow solid (1.42 g, 81%). ^{1}H NMR (CD_2Cl_2, 400 MHz): δ 8.67 (d, 2H, J = 2 Hz), 7.94 (t, 1H, J = 2 Hz), 7.62−7.66 (br s, 8H), 7.36−7.38 (br s, 12H); ^{31}P NMR ($CDCl_3$, 202.468 MHz): δ −34.06. ESI-MS(+) m/z calcd. for $[M+H]^+$: 496.14, found $[M+H]^+$: 496.24.

1,5-Diiodonaphthalene (7). A previously reported procedure was used for the preparation of 1,5-diiodonaphthalene.[31] To a solution of sodium nitrite (3.0 g, 0.044 mol) in concentrated sulfuric acid (25 mL) at 0 °C was added to a solution of 1,5-diaminonaphthalene (3 g, 0.019 mol) in glacial acetic acid (25 mL). The mixture was stirred for 15 min followed by addition of ice (50 g) and urea (0.25 g). A solution of KI (100 g, 0.6 mol) in water (100 mL) was added and stirred overnight under house vacuum. The solvent evaporated overnight leaving a solid residue, which was washed with CH_2Cl_2 (3 × 100 mL). The combined CH_2Cl_2 washes were refluxed with decolorizing charcoal, filtered through a Celite-layered glass filter, and purified by silica gel column chromatography (eluting with hexane/dichloromethane (2:1)) to give **7** as pale-yellow powder (3.68 g, 51%). ^{1}H NMR ($CDCl_3$, 400 MHz): δ 8.14 (m, 4H), 7.28 (dd, 2H, J = 16 Hz, 7.6 Hz). ^{13}C NMR ($CDCl_3$, 200 MHz): δ 138.87 (2C), 134.79 (2C), 133.78 (2C), 128.69 (2C), 99.76 (2C). ESI-MS(+) m/z calcd. for $[M]^+$: 379.9, found $[M]^+$: 380.0, calcd. for $[M-I]^+$: 253.0, found $[M]^+$: 253.0, calcd. for $[M-2I+H]^+$: 126.0, found $[M-2I+H]^+$: 126.2.

1,5-Bis((trimethylsilyl)ethynyl)naphthalene (8). Compound **7** (0.76 g, 2 mmol) was dissolved in diethylamine (20 mL) under an atmosphere of nitrogen. CuI (19 mg, 2.5 mol %) and $PdCl_2(PPh_3)_2$ (42 mg, 1.5 mol %) were added to the solution. Trimethylsilylacetylene (0.7 mL, 2.4 mmol) was slowly added, and the mixture was heated to reflux for 12 h. Once conversion was complete (by TLC), the solvent was evaporated. The mixture was separated by silica gel column chromatography (n-hexane) to isolate the title compound (0.49 g, 76%). ^{1}H NMR ($CDCl_3$, 400 MHz): δ 8.35 (d, 2H, J = 8 Hz), 7.74 (d, 2H, J = 8 Hz), 7.52 (t, 2H, J = 8 Hz), 0.34 (s, 18H).

1,5-Diethynylnaphthalene (9). Compound **8** (0.48 g, 1.5 mmol) was dissolved in 10 mL of CH_2Cl_2, followed by adding a mixture of MeOH/NaOH (10 mL/0.75 g). The mixture was stirred for 12 h at room temperature. Once conversion was complete (by TLC), the solvent was evaporated. Thirty milliliters of CH_2Cl_2 was added to the residue, and the insoluble solids were filtered away. The filtrate was washed with brine (2 × 30 mL) and then the organic phase was separated and dried with Na_2SO_4. After removing the solvent, the solid mixture was separated by silica gel column chromatography using CH_2Cl_2 as eluent to give the title compound (0.246 g, 93%). ^{1}H NMR ($CDCl_3$, 400 MHz): δ 8.39 (d, 2H, J = 8 Hz), 7.78 (d, 2H, J = 8 Hz), 7.53 (t, 2H, J = 8 Hz), 3.49 (s, 2H); ESI-MS (+) m/z calcd. for $[M+MeOH+H]^+$: 129.10, found $[M+MeOH+H]^+$: 209.11, calcd. for $[M+2MeOH+H]^+$: 241.13, found $[M+MeOH+H]^+$: 241.09.

1,5-Bis((diphenylphosphino)ethynyl)naphthalene (L^5). Compound **9** (0.25 g, 1.42 mmol) was dissolved in freshly dried THF (30 mL) at −20 °C. ^{n}BuLi (2.5 M hexane, 1.4 mL, 3.5 mmol) was slowly added to the solution. The reaction mixture was stirred for 30 min, and then Ph_2PCl (0.6 mL, 3.5 mmol) was added and stirred for an additional 2 h. Once the reaction was complete (by TLC), the solvent was evaporated, and the residue dissolved in CH_2Cl_2 (30 mL). The organic layer was washed with water (3 × 20 mL). After drying with Na_2SO_4, the solvent was removed in a vacuum to yield a yellow solid (0.58 g, 75%). ^{1}H NMR (CD_2Cl_2, 400 MHz): δ 8.35 (d, 2H, J = 8 Hz), 7.81 (d, 2H, J = 8 Hz), 7.72−7.76 (br s, 8H), 7.51 (t, 2H, J = 8 Hz), 7.38−7.40 (br s, 12H); ^{31}P NMR ($CDCl_3$, 202.468 MHz): δ −33.57. ESI-MS(+) m/z calcd. for $[M+H]^+$: 545.16, found $[M+H]^+$: 545.38, $[M+MeOH+H]^+$: 577.19, found $[M+MeOH+H]^+$: 577.25.

$Cu_4(L^1)_4I_4$. CuI (38 mg, 0.2 mmol) was suspended in CH_2Cl_2 (50 mL), and L^1 (190 mg, 0.2 mmol) was added. The solution was stirred for 30 min producing a clear solution. The solution was filtered, and the solvent removed in vacuum. The pale yellow solid was collected and washed with Et_2O (212 mg, 93%). Crystals suitable for X-ray structure determination were grown from slow diffusion of Et_2O into a saturated solution of the material in CH_2Cl_2 giving colorless block-shaped crystals within a couple days (170 mg, 80% yield from the isolated powder). ^{31}P NMR (CD_2Cl_2, 202.468 MHz): δ 7.73. High resolution ESI-MS(+) m/z: calcd. for $[M-I]^+$ 4358.5319, found $[M-I]^+$ 4358.5331, calcd. for $[M+Na]^+$ 4508.4261, found $[M+Na]^+$ 4508.4298.

$Ag_4(L^1)_4I_4$. AgI (47 mg, 0.2 mmol) was suspended in CH_2Cl_2 (50 mL), and L^1 (190 mg, 0.2 mmol) was added. The solution was stirred for 30 min producing a clear solution. The solution was filtered, and the solvent removed in vacuum. The pale yellow solid was collected and washed with Et_2O (219 mg, 94%). Crystals suitable for X-ray structure determination were grown from slow diffusion of Et_2O into a saturated solution of the material in CH_2Cl_2 giving colorless block-shaped crystals within a couple of days (180 mg, 82% yield from the isolated powder). ^{1}H NMR (CD_2Cl_2, 500 MHz): δ 7.87(br s, 24H), 7.75 (br s, 24H), 7.66 (t, 12H, J = 9 Hz), 7.35 (br s, 24H), 7.29 (s, 12H), 7.22 (t, 12H, J = 8 Hz), 7.14 (d, 24H, J = 8.5 Hz), 7.01 (t, 24H, J = 8.5 Hz), 6.87 (d, 24H, J = 8.5 Hz); ^{31}P NMR (CD_2Cl_2, 202.468 MHz): δ - 31.38 ($^1J(^{107}Ag-P)$ = 246 Hz and $^1J(^{109}Ag-P)$ = 284 Hz).

$Au_4(L^1)_4I_4$. AuI (65 mg, 0.2 mmol) was suspended in CH_2Cl_2 (50 mL), and L^1 (190 mg, 0.2 mmol) was added. The solution was stirred for 30 min producing a clear solution. The solution was filtered, and the solvent removed in a vacuum. The pale yellow solid was collected and washed with Et_2O (225 mg, 88%). Crystals suitable for X-ray structure determination were grown from slow diffusion of Et_2O into a saturated solution of the material in CH_2Cl_2 giving colorless block-shaped crystals within a couple days (171 mg, 76% yield from the isolated powder). ^{31}P NMR (CD_2Cl_2, 202.468 MHz): δ 7.99.

$Cu_2(L^2)_3I_2$. CuI (38 mg, 0.2 mmol) was suspended in CH_2Cl_2 (50 mL) and L^2 (150 mg, 0.3 mmol) was added. The solution was stirred for 30 min producing a clear solution. The solution was filtered, and the solvent removed in a vacuum. The yellow solid was collected and washed with Et_2O (179 mg, 95%). Crystals suitable for X-ray structure determination were grown from slow diffusion of Et_2O into a saturated solution of the material in CH_2Cl_2 giving colorless block-shaped crystals within a couple days (161 mg, 90% yield from the isolated powder). ^{1}H NMR (CD_2Cl_2, 400 MHz): δ 7.77 (br s, 24H), 7.18 (t, 12H, J = 8 Hz), 7.13 (s, 12H), 7.08 (t, 24H, J = 8 Hz); ^{31}P NMR

dx.doi.org/10.1021/ic302840x | Inorg. Chem. XXXX, XXX, XXX−XXX

(CD_2Cl_2, 202.468 MHz): δ 9.84; High resolution ESI-MS(+) m/z: calcd. for $[M-I]^+$ 1737.1708, found $[M-I]^+$ 1737.1703, calcd. for $[M+Na]^+$ 1887.0650, found $[M+Na]^+$ 1887.0631, calcd. for $[M+K]^+$ 1903.0388, found $[M+K]^+$ 1903.0631, calcd. for $[M+Cu]^+$ 1927.0040, found $[M+Cu]^+$ 1927.0060.

$Cu_2(L^3)_3I_2$. CuI (92 mg, 0.24 mmol) was suspended in CH_2Cl_2 (50 mL) and L^3 (180 mg, 0.36 mmol) was added. The solution was stirred for 30 min producing a clear solution. The solution was filtered and the solvent removed in a vacuum. The yellow solid was collected and washed with Et_2O (260 mg, 96%). Crystals suitable for X-ray structure determination were grown from slow diffusion of Et_2O into a saturated solution of the material in CH_2Cl_2 giving colorless crystals within two weeks (182 mg, 70% yield from the isolated powder). ^1H NMR (CD_2Cl_2, 400 MHz): δ 7.80 (br s, 24H), 7.30 (t, 12H, J = 8 Hz), 7.19 (t, 3H, J = 8 Hz), 7.16 (t, 24H, J = 8 Hz), 6.76 (d, 6H, J = 8 Hz), 5.64(s, 3H); ^{31}P NMR (CD_2Cl_2, 202.468 MHz): δ 7.53; High resolution ESI-MS(+) m/z: calcd. for $[M-I]^+$ 1737.1708, found $[M-I]^+$ 1737.1673, calcd. for $[M+Na]^+$ 1887.0650, found $[M+Na]^+$ 1887.0631.

$Cu_2(L^4)_3I_2$. CuI (26 mg, 0.135 mmol) was suspended in CH_2Cl_2 (30 mL) and L^4 (100 mg, 0.2 mmol) was added. The solution was stirred for 30 min producing a clear solution. The solution was filtered, and the solvent removed in a vacuum. The yellow solid was collected and washed with Et_2O (117 mg, 93%). Crystals suitable for X-ray structure determination were grown from slow diffusion of Et_2O into a saturated solution of the material in CH_2Cl_2 giving colorless block-shaped crystals within a couple days (112 mg, 96% yield from the isolated powder). ^1H NMR (CD_2Cl_2, 400 MHz): δ 8.02 (d, 6H, J = 2 Hz), 7.83 (br s, 24H), 7.37 (t, 12H, J = 8 Hz), 7.22 (t, 24H, J = 8 Hz), 5.78 (t, 3H, J = 2 Hz); ^{31}P NMR (CD_2Cl_2, 202.468 MHz): δ 9.64; High resolution ESI-MS(+) m/z: calcd. for $[M-I]^+$ 1740.1607, found $[M-I]^+$ 1740.1607, calcd. for $[M+Na]^+$ 1889.05, found $[M+Na]^+$ 1890.0528.

$Au_2(L^4)_3I_2$. AuI (44 mg, 0.135 mmol) was suspended in CH_2Cl_2 (30 mL), and L^4 (100 mg, 0.2 mmol) was added. The solution was stirred for 30 min producing a clear solution. The solution was filtered, and the solvent removed in a vacuum. The yellow solid was collected and washed with Et_2O (121 mg, 84%). Crystals suitable for X-ray structure determination were grown from slow diffusion of Et_2O into a saturated solution of the material in CH_2Cl_2 giving yellow hexagonal plates within 2 days (115 mg, 95% yield from the isolated powder). ^1H NMR (CD_2Cl_2, 400 MHz): δ 8.43 (d, 6H, J = 2.4 Hz), 7.78 (m, 24H), 7.41 (m, 12H), 7.37 (m, 24H), 7.34 (t, 3H, J = 2.4 Hz); ^{31}P NMR (CD_2Cl_2, 202.468 MHz): δ 10.06.

$[Au_2(L^2)_3I_2]_n$. AuI (65 mg, 0.2 mmol) was suspended in CH_2Cl_2 (50 mL), and L^2 (150 mg, 0.3 mmol) was added. The solution was stirred for 30 min producing a clear solution. The solution was filtered and the solvent removed in a vacuum. The yellow solid was collected and washed with Et_2O (172 mg, 80%). Crystals suitable for X-ray structure determination were grown from slow diffusion of Et_2O into a saturated solution of the material in CH_2Cl_2 giving colorless needle-shaped crystals within two weeks (112 mg, 65% yield from the isolated powder). ^{31}P NMR (CD_2Cl_2, 202. 468 MHz): δ 7.63.

$[Cu_2(L^5)_3I_2]_n$. CuI (38 mg, 0.2 mmol) was suspended in CH_2Cl_2 (50 mL), and L^5 (164 mg, 0.3 mmol) was added. The solution was stirred for 30 min producing a clear solution. The solution was filtered, and the solvent removed in vacuum. The yellow solid was collected and washed with Et_2O (170 mg, 84%). Colorless block-shaped crystals suitable for X-ray structure determination were grown from saturated (hot) DMF solution upon cooling overnight (119 mg, 70% yield from the isolated powder). ^{31}P NMR (CD_2Cl_2, 202.468 MHz): δ 6.61.

Mass Spectrometry Analysis. High-resolution electrospray ionization mass spectrometry (ESI-MS) was performed using an Agilent 6230 ESI-TOFMS mass spectrometer, and the data was analyzed using the Agilent MassHunter software suite. Samples were dissolved in CH_2Cl_2 and diluted with acetone. Acetone was used as the working flow to carry the diluted sample to the ESI source.

Single Crystal X-ray Diffraction. Single crystals from the mother liquor were mounted on nylon loops with Paratone oil and placed under a nitrogen cold stream (100 K). Data were collected on a Bruker Apex diffractometer using either Cu Kα radiation or Mo Kα radiation controlled using the APEX 2010 software package. A semiempirical method utilizing equivalents was employed to correct for absorption. Hydrogen atoms were added geometrically and refined with a riding model. All structures were solved by direct methods with SIR 2004[32] and refined by full-matrix least-squares procedures utilizing SHELXL-97.[33] Crystallographic data collection and refinement information is listed in Supporting Information,Table S1−S3. Most of the crystals diffracted very weakly and are fragile upon exposure to air, leading to some loss in crystallinity. As a result, some of crystals, including CH_2Cl_2@$Cu_4(L^1)_4I_4$, CH_2Cl_2@$Ag_4(L^1)_4I_4$, DMF@$Ag_4(L^1)_4I_4$, CH_2Cl_2@$Au_4(L^1)_4I_4$, and $Cu_2(L^3)_3I_2$) never reached 100% completeness despite several attempts at data collection. Most of the Alert Level A warnings in the checkCIF file come from this incompleteness. In addition, many of the crystal structures contained a number of phenyl-group positional disorders, which were extensively restrained using EADP and AFIX 66, and were refined anisotropically. For further refinement, the carbon atoms on disordered phenyl groups were split into two positions, which were also restrained using EADP and refined anisotropically. The crystallographic routine SQUEEZE[34] was used to account for disordered solvent molecules, which found 747, 258, 246, 323, 169, and 156 electrons per void volume (Å^3) for CH_2Cl_2@$Cu_4(L^1)_4I_4$, CH_2Cl_2@$Ag_4(L^1)_4I_4$, DMF@$Ag_4(L^1)_4I_4$, CH_2Cl_2@$Au_4(L^1)_4I_4$, $Cu_2(L^4)_3I_2$, and $Au_2(L^4)_3I_2$, respectively. The other structures reported here, $Cu_2(L^2)_3I_2$, $Cu_2(L^3)_3I_2$, $[Au_2(L^2)_3I_2]_n$, and $[Cu_2(L^5)_3I_2]_n$, were refined without the use of the SQUEEZE protocol.

■ ASSOCIATED CONTENT

Ⓢ Supporting Information

Cystallographic data in CIF format. Further details are given in Schemes S1−S2, Figures S1−S16, and Tables S1−S6. This material is available free of charge via the Internet at http://pubs.acs.org.

■ AUTHOR INFORMATION

Corresponding Author

*E-mail: scohen@ucsd.edu. Phone: (858) 822-5596.

Notes

The authors declare no competing financial interest.

■ ACKNOWLEDGMENTS

We thank Dr. David Puerta, Dr. Jean-Philippe Monserrat, Mr. Phuong Dau, Mr. Kevin B. Daniel, and Mr. Joshua A. Day (UCSD) for critical reading of this manuscript. We also thank Dr. Yongxuan Su (UCSD) for assistance with ESI-MS and Dr. Moore Curtis (UCSD) for assistance with the refinement of the X-ray crystal structures. This work was supported by a grant from the Department of Energy (BES Grant DE-FG02-08ER46519).

■ DEDICATION

Dedicated to Prof. Kenneth N. Raymond on the occasion of his 70th birthday.

■ REFERENCES

(1) (a) Caulder, D. L.; Raymond, K. N. *Acc. Chem. Res.* **1999**, *32*, 975. (b) Leininger, S.; Olenyuk, B.; Stang, P. J. *Chem. Rev.* **2000**, *100*, 853. (c) Fujita, M.; Tominaga, M.; Hori, A.; Therien, B. *Acc. Chem. Res.* **2005**, *38*, 369. (d) Chakrabarty, R.; Mukherjee, P. S.; Stang, P. J. *Chem. Rev.* **2011**, *111*, 6810.

(2) (a) Meyer, M.; Kersting, B.; Powers, R. E.; Raymond, K. N. *Inorg. Chem.* **1997**, *36*, 5179. (b) Caulder, D. L.; Raymond, K. N. *Angew. Chem., Int. Ed.* **1997**, *36*, 1439. (c) Scherer, M.; Caulder, D. L.; Johnson, D. W.; Raymond, K. N. *Angew. Chem., Int. Ed.* **1999**, *38*, 1588. (d) Yeh, R. M.; Raymond, K. N. *Inorg. Chem.* **2006**, *45*, 1130.

(e) Uerpmann, C.; Malina, J.; Pascu, M.; Clarkson, G. J.; Moreno, V.; Rodger, A.; Grandas, A.; Hannon, M. J. *Chem.—Eur. J.* **2005**, *11*, 1750. (f) Albrecht, M.; Liu, Y.; Zhu, S. S.; Schalley, C. A.; Fröhlich, R. *Chem. Commun.* **2009**, 1195. (g) Schultz, D.; Biaso, F.; Shahi, A. R. M.; Geoffroy, M.; Rissanen, K.; Gagliardi, L.; Cramer, C. J.; Nitschke, J. R. *Chem.—Eur. J.* **2008**, *14*, 7180.

(3) (a) Saalfrank, R. W.; Burak, R.; Breit, A.; Stalke, D.; Herbst-Irmer, R.; Daub, J.; Porsch, M.; Bill, E.; Müther, M.; Trautwein, A. X. *Angew. Chem., Int. Ed.* **1994**, *33*, 1621. (b) Caulder, D. L.; Powers, R. E.; Parac, T.; Raymond, K. N. *Angew. Chem., Int. Ed.* **1998**, *37*, 1840. (c) Leininger, S.; Fan, J.; Schmitz, M.; Stang, P. J. *Proc. Natl. Acad. Sci.* **2000**, *97*, 1380. (d) Meng, W.; Clegg, J. K.; Thoburn, J. D.; Nitschke, J. R. *J. Am. Chem. Soc.* **2011**, *133*, 13652.

(4) (a) Hiraoka, S.; Harano, K.; Shiro, M.; Ozawa, Y.; Yasuda, N.; Toriumi, K.; Shionoya, M. *Angew. Chem., Int. Ed.* **2006**, *45*, 6488. (b) Harano, K.; Hiraoka, S.; Shionoya, M. *J. Am. Chem. Soc.* **2007**, *129*, 5300. (c) Ronson, T. K.; Fisher, J.; Harding, L. P.; Hardie, M. J. *Angew. Chem., Int. Ed.* **2007**, *46*, 9086.

(5) (a) Paquette, L. A.; Balogh, D. W.; Usha, R.; Kountz, D.; Christoph, G. G. *Science* **1981**, *211*, 575. (b) Olenyuk, B.; Levin, M. D.; Whiteford, J. A.; Shield, J. E.; Stang, P. J. *J. Am. Chem. Soc.* **1999**, *121*, 10434. (c) Levin, M. D.; Stang, P. J. *J. Am. Chem. Soc.* **2000**, *122*, 7428.

(6) (a) Olenyuk, B.; Whiteford, J. A.; Fechtenkötter, A.; Stang, P. J. *Nature* **1999**, *398*, 796. (b) Atwood, J. L.; Barbour, L. J.; Dalgarno, S. J.; Hardie, M. J.; Raston, C. L.; Webb, H. R. *J. Am. Chem. Soc.* **2004**, *126*, 13170. (c) Argent, S. P.; Adams, H.; Riis-Johannessen, T.; Jefferey, J. C.; Harding, L. P.; Ward, M. D. *J. Am. Chem. Soc.* **2006**, *128*, 72. (d) Ghosh, K.; Hu, J.; White, H. S.; Stang, P. J. *J. Am. Chem. Soc.* **2009**, *131*, 6695. (e) Li, D.; Zhou, W.; Landskron, K.; Sato, S.; Kiely, C. J.; Fujita, M.; Liu, T. *Angew. Chem., Int. Ed.* **2011**, *50*, 5182.

(7) (a) Zheng, Y.-R.; Ghosh, K.; Yang, H.-B.; Stang, P. J. *Inorg. Chem.* **2010**, *49*, 4747. (b) Kelley, R. F.; Lee, S. J.; Wilson, T. M.; Nakamura, Y.; Tiede, D. M.; Osuka, A.; Hupp, J. T.; Wasielewski, M. R. *J. Am. Chem. Soc.* **2008**, *130*, 4277. (c) Caskey, D. C.; Yamamoto, T.; Addicott, C.; Shoemaker, R. K.; Vacek, J.; Hawkridge, A. M.; Muddiman, D. C.; Kottas, G. S.; Michl, J.; Stang, P. J. *J. Am. Chem. Soc.* **2008**, *130*, 7620. (d) Hong, M.; Zhao, y.; Su, W.; Cao, R.; Fujita, M.; Zhou, Z.; Chan, A. S. C. *J. Am. Chem. Soc.* **2000**, *122*, 4819.

(8) (a) Fiedler, D.; Leung, D. H.; Bergman, R. G.; Raymond, K. N. *J. Am. Chem. Soc.* **2004**, *126*, 3674. (b) Davis, A. V.; Fiedler, D.; Seeber, G.; Zahl, A.; van Eldik, R.; Raymond, K. N. *J. Am. Chem. Soc.* **2006**, *128*, 1324. (c) Leung, D. H.; Bergman, R. G.; Raymond, K. N. *J. Am. Chem. Soc.* **2008**, *130*, 2798. (d) Pluth, M. D.; Tiedemann, B. E. F.; van Halbeek, H.; Nunlist, R.; Raymond, K. N. *Inorg. Chem.* **2008**, *47*, 1411. (e) Kusukawa, T.; Fujita, M. *J. Am. Chem. Soc.* **2002**, *124*, 13576. (f) Sun, W.; Kusukawa, T.; Fujita, M. *J. Am. Chem. Soc.* **2002**, *124*, 11570. (g) Murase, T.; Otsuka, K.; Fujita, M. *J. Am. Chem. Soc.* **2010**, *132*, 7864. (h) Mal, P.; Schultz, D.; Beyeh, K.; Rissanen, K.; Nitschke, J. R. *Angew. Chem., Int. Ed.* **2008**, *47*, 8297. (i) Ousaka, N.; Clegg, J. K.; Nitschke, J. R. *Angew. Chem., Int. Ed.* **2012**, *51*, 1464.

(9) (a) Ziegler, M.; Brumaghim, J. L.; Raymond, K. N. *Angew. Chem., Int. Ed.* **2000**, *39*, 4119. (b) Fiedler, D.; Bergman, R. G.; Raymond, K. N. *Angew. Chem., Int. Ed.* **2006**, *45*, 745. (c) Kawano, M.; Kobayashi, Y.; Ozeki, T.; Fujita, M. *J. Am. Chem. Soc.* **2006**, *128*, 6558. (d) Mal, P.; Breiner, B.; Rissanen, K.; Nitschke, J. R. *Science* **2009**, *324*, 1697.

(10) (a) Brown, C. J.; Bergman, R. G.; Raymond, K. N. *J. Am. Chem. Soc.* **2009**, *131*, 17530. (b) Fiedler, D.; van Halbeek, H.; Bergman, R. G.; Raymond, K. N. *J. Am. Chem. Soc.* **2006**, *128*, 10240. (c) Pluth, M. D.; Bergman, R. G.; Raymond, K. N. *J. Am. Chem. Soc.* **2008**, *130*, 8587. (d) Wang, Z. J.; Brown, C. J.; Bergman, R. G.; Raymond, K. N.; Toste, F. D. *J. Am. Chem. Soc.* **2011**, *133*, 7358. (e) Noh, T. H.; Heo, E.; Parl, K. H.; Jung, O.-S. *J. Am. Chem. Soc.* **2011**, *133*, 1236. (f) Smulders, M. M. J.; Maarten, M. J.; Nitschke, J. R. *Chem. Sci.* **2012**, *3*, 785.

(11) Kreickmann, T.; Diedrich, C.; Pape, T.; Hyunh, H. V.; Grimme, S.; Hahn, F. E. *J. Am. Chem. Soc.* **2006**, *128*, 11808.

(12) Birkmann, B.; Fröhlich, R.; Hahn, F. E. *Chem.—Eur. J.* **2009**, *15*, 9325.

(13) Hahn, F. E.; Isfort, C. S.; Pape, T. *Angew. Chem., Int. Ed.* **2004**, *43*, 4807.

(14) (a) Rit, A.; Pape, T.; Hahn, F. E. *J. Am. Chem. Soc.* **2010**, *132*, 4572. (b) Rit, A.; Pape, T.; Hepp, A.; Hahn, F. E. *Organometallics* **2011**, *30*, 334.

(15) (a) Cangelosi, V. M.; Sather, A. C.; Zakharov, L. N.; Berryman, O. B.; Johnson, D. W. *Inorg. Chem.* **2007**, *46*, 9278. (b) Cangelosi, V. M.; Zakharov, L. N.; Johnson, D. W. *Angew. Chem., Int. Ed.* **2010**, *49*, 1248.

(16) (a) Osborn, J. A.; Jardine, F. H.; Young, J. F.; Wilkinson, G. *J. Chem. Soc. A* **1966**, 1711. (b) Hidai, M.; Tominari, K.; Uchida, Y. *J. Am. Chem. Soc.* **1972**, *94*, 110. (c) Grubbs, R. H. *Adv. Synth. Catal.* **2007**, *349*, 34.

(17) James, S. L. *Chem. Soc. Rev.* **2009**, *38*, 1744.

(18) (a) Puddephatt, R. J. *Chem. Soc. Rev.* **2008**, *37*, 2012. (b) Yip, J. H. K.; Prabhavathy, J. *Angew. Chem., Int. Ed.* **2001**, *40*, 2159. (c) James, S. L.; Mingos, D. M. P.; White, A. J. P.; Williams, D. J. *Chem. Commun.* **1998**, 2323. (d) Lim, S. H.; Olmstead, M. M.; Balch, A. L. *Chem. Sci.* **2013**, *4*, 311. (e) Sun, X.; Johnson, D. W.; Caulder, D. L.; Raymond, K. N.; Wong, E. H. *J. Am. Chem. Soc.* **2001**, *123*, 2752.

(19) Lim, S. H.; Olmstead, M. M.; Balch, A. L. *J. Am. Chem. Soc.* **2011**, *133*, 10229.

(20) Macgregor, S. A. *Chem, Soc. Rev.* **2007**, *36*, 67.

(21) Lim, S. H.; Su, Y.; Cohen, S. M. *Angew. Chem., Int. Ed.* **2012**, *51*, 5106.

(22) Weber, E.; Hecker, M.; Koepp, E.; Orlia, W. *J. Chem. Soc., Perkin Trans. 2* **1988**, 1251.

(23) Constable, E. C.; Housecroft, C. E.; Krattinger, B.; Neuburger, M.; Zehnder, M. *Organometallics* **1999**, *18*, 2565.

(24) Based on the Cambridge Structural Database (CSD), the average bond distances of M(I)-phosphine and M(I)-iodide (M = Cu, Ag, and Au) in other four-coordinate phosphine-based metal(I) iodide complexes are ~2.30, 2.54, and ~2.40 Å for Cu-P, Ag-P, and Au-P, and ~2.65, ~2.84, and ~2.94 Å for Cu-I, Ag-I, and Au-I, respectively.

(25) To get the cavity volumes of the tetrahedral clusters $M_4(L^1)_4I_4$ ($M = Cu^+$, Ag^+, and Au^+), the average distance from the centroid of the overall cluster to the centroids of the central benzene of each ligand of the cluster was obtained from the crystal structure data. This value provides an estimation of the radii for a sphere that fits in the cavity, from which the empty cavity volume was estimated.

(26) (a) Yau, J.; Mingos, D. M. P. *J. Chem. Soc., Dalton Trans.* **1997**, 1103. (b) Lim, S. H.; Schmitt, J. C.; Shearer, J.; Jia, J.; Olmstead, M. M.; Fettinger, J. C.; Balch, A. L. *Inorg. Chem.* **2013**, *52*, 823. (c) Effendy; Nicola, C. D.; Fianchini, M.; Pettinari, C.; Skelton, B. W.; Somers, N.; White, A. H. *Inorg. Chim. Acta* **2005**, *358*, 763.

(27) (a) Nunokawa, K.; Onaka, S.; Tatematsu, T.; Ito, T.; Sakai, J. *Inorg. Chim. Acta* **2001**, *322*, 56. (b) Muetterties, E. L.; Alegranti, C. W. *J. Am. Chem. Soc.* **1972**, 6383.

(28) Lozano, E.; Nieuwenhuyzen, M.; James, S. L. *Chem.—Eur. J.* **2001**, *7*, 2644.

(29) Pluth, M. D.; Raymond, K. N. *Chem. Soc. Rev.* **2007**, *36*, 161.

(30) Gorin, D. J.; Toste, F. D. *Chem. Soc. Rev.* **2008**, 3351.

(31) Rodríguez, J. G.; Tejedor, J. L. *J. Org. Chem.* **2002**, *67*, 7631.

(32) Burla, M. C.; Caliandro, R.; Camalli, M.; Carrozzini, B.; Cascarano, G. L.; De Caro, L.; Gaicovazzo, C.; Polidori, G.; Spagna, R. *J. Appl. Crystallogr.* **2005**, *38*, 381.

(33) Sheldrick, G. M. *Acta Crystallogr.* **2008**, *A64*, 112.

(34) van der Sluis, P.; Spek, A. L. *Acta Crystallogr.* **1990**, *A46*, 194.

dx.doi.org/10.1021/ic302840x | *Inorg. Chem.* XXXX, XXX, XXX–XXX